

The tensor-optimized high-momentum antisymmetrized molecular dynamics with bare interaction and its application in ${}^4\text{He}$ nucleus

Mengjiao Lyu,^{1,*} Takayuki Myo,^{2,1,†} Masahiro Isaka,³ Hiroshi Toki,¹
Kiyomi Ikeda,⁴ Hisashi Horiuchi,¹ Tadahiro Suhara,⁵ and Taiichi Yamada⁶

¹*Research Center for Nuclear Physics (RCNP),
Osaka University, Ibaraki, Osaka 567-0047, Japan*

²*General Education, Faculty of Engineering,
Osaka Institute of Technology, Osaka, Osaka 535-8585, Japan*

³*Hosei University, 2-17-1 Fujimi, Chiyoda-ku, Tokyo 102-8160, Japan*

⁴*RIKEN Nishina Center, Wako, Saitama 351-0198, Japan*

⁵*Matsue College of Technology, Matsue 690-8518, Japan*

⁶*Laboratory of Physics, Kanto Gakuin University, Yokohama 236-8501, Japan*

(Dated: October 16, 2018)

Abstract

We formulate the “tensor-optimized high-momentum antisymmetrized molecular dynamics (TO-HMAMD)” framework for *ab initio* calculations of nuclei by hybridizing the tensor-optimized (TO-) and high-momentum (HM-) AMD approaches. This hybrid approach has advantages in both analytical simplicity and numerical efficiency comparing with other AMD-based methods which treat the bare interaction, especially for heavier nuclear systems. In this work, the *s*-shell nucleus ${}^4\text{He}$ is calculated with TO-HMAMD by including up to double product of nucleon-nucleon (NN) correlations, described by using high-momentum pairs and spatial correlation functions of nucleons. The total energy and radius of the ${}^4\text{He}$ nucleus are well reproduced using the AV8' interaction. The spin-isospin channel dependence is also discussed for NN -correlations, which are found to be mostly contributed in the even-state channels, especially the triplet-even channel. Analyses of the analytical formation and numerical results suggest that TO-HMAMD could be a promising framework for *p*-shell nuclear systems.

* mengjiao@rcnp.osaka-u.ac.jp

† takayuki.myo@oit.ac.jp

I. INTRODUCTION

The bare nucleon-nucleon (NN) interaction has been determined phenomenologically in high precision by reproducing the NN scattering data [1]. In recent years, it is in active progress to predict the NN interaction from the underlying Quantum Chromodynamics (QCD) [2]. The strong tensor force and short-range repulsion in the bare NN interaction have been observed in both phenomenological models and the underlying field theory. In nuclei, strong NN -correlations, including tensor and short-range correlations, are induced by tensor force and short-range repulsion, respectively [3]. In *ab initio* calculations, an accurate description of NN correlations is crucial for both the exact solution of nuclear wave functions and the examinations of the underlying QCD predictions for nucleon systems. Usually, in *ab initio* calculations, correlation functions based on the Jastrow type or unitary transformation with the exponential form are multiplied to the reference nuclear state [1, 4].

In the present and previous works [5], we propose the “tensor-optimized high-momentum antisymmetrized molecular dynamics” (TO-HMAMD) for *ab initio* calculations of nuclear system, which is a hybridization of the “tensor-optimized antisymmetrized molecular dynamics” (TOAMD) method [6–10] and the “high-momentum antisymmetrized molecular dynamics” (HMAMD) method [11–13]. These three methods are based on the framework of “antisymmetrized molecular dynamics” (AMD), which has been very successful in microscopic description of light nuclei, especially for the cluster states [14, 15]. In the TOAMD approach, the variational correlation functions in operator forms are explicitly formulated for both central and tensor channels and then their multiple products successively act on the AMD basis state. The TOAMD method is applied in *ab initio* calculations of s -shell nuclei by using the AV8’ bare interaction, and reproduces well the total energies and radii of ${}^3\text{H}$ and ${}^4\text{He}$ nuclei [7]. In Ref. [10], it is found that using the AV6 interaction, the TOAMD wave function provides better energies for s -shell nuclei comparing with the variational wave functions with the Jastrow type NN -correlations. In the HMAMD approach, the NN correlations are directly described by using the NN -pairs with large momenta in their relative motion [11, 12], which are called “high-momentum pairs”. With these high-momentum pairs both of the tensor and short-range correlations can be described satisfactorily. This approach is similar to the one used in *i*SMT [16] and AQCM-T [17], in which the tensor correlation is treated. In Ref. [12], energies and radii of the ${}^3\text{H}$ nucleus are calculated

through the HMAMD approach using multi high-momentum pairs and the AV4' central interaction having short-range repulsions. It is found that the solutions obtained in TOAMD and HMAMD approaches converge exactly with each other and nicely reproduce the Green's function Monte Carlo results [12].

From the convergence behavior of the solutions for light nuclei between TOAMD and HMAMD, it is concluded that the correlation function in the TOAMD method and the high-momentum NN pairs in the HMAMD method essentially describe the same NN correlations [12]. However, there are differences of both physical concepts and mathematical expressions between these two methods. If these two methods are combined, we expect to get a better description of many-body correlations in *ab initio* studies of nuclei, where many kinds of NN correlations can be included in the wave function. We try to integrate the analytical simplicity of the HMAMD approach and numerical efficiency of the TOAMD approach. Hence, the hybridized nature of TO-HMAMD could be a promising framework for p -shell nuclear system. In our previous work, we have applied the TO-HMAMD method to the *ab initio* calculation of the simple ^3H nucleus, and discussed the accuracy and flexibility of the method. In this work, we perform the detailed comparison of the formulations of TO-HMAMD with those of HMAMD and TOAMD, and apply the TO-HMAMD method to *ab initio* calculations of much more complicated nuclei ^4He using the AV8' bare interaction.

This paper is organized as follows. In Sec. II, we introduce the cluster expansion of the multiple products of the NN -correlations. We also explain the HMAMD and TOAMD methods and finally the formulation of the hybridized TO-HMAMD approach. We discuss in detail the advantages of the TO-HMAMD method in comparison with HMAMD and TOAMD. In Sec. III, we present the numerical results and discussions of the *ab initio* calculations for the ^4He nucleus by using the TO-HMAMD method. In Sec. IV, we discuss the spin-isospin channel dependence of NN -correlations in the wave function of TO-HMAMD. The last Sec. V contains the conclusion.

II. FORMULATION

We introduce the framework of TO-HMAMD by explaining first the AMD wave function and next the cluster expansion of the products of NN -correlations, and then formulate successively HMAMD, TOAMD and TO-HMAMD approaches.

A. Antisymmetrized Molecular Dynamics (AMD)

These HMAMD, TOAMD and TO-HMAMD methods are based on the AMD wave function which is defined as the Slater determinant of A -nucleon system,

$$|\Phi_{\text{AMD}}\rangle = \det\{|\phi_1(\mathbf{r}_1) \cdots \phi_A(\mathbf{r}_A)\rangle\}. \quad (1)$$

Here, the single-nucleon states $\phi(\mathbf{r})$ are expressed in the Gaussian wave packet form with the range parameter ν and the centroid \mathbf{R} multiplied by the spin-isospin component $\chi_{\tau,\sigma}$,

$$\phi(\mathbf{r}) \propto e^{-\nu(\mathbf{r}-\mathbf{R})^2} \chi_{\tau,\sigma}. \quad (2)$$

The Gaussian centroids \mathbf{R} are usually determined by the cooling process as discussed in Refs. [14, 15]. For s -shell nuclei ${}^3\text{H}$ and ${}^4\text{He}$, the centroids are optimized to be $\mathbf{R} = \mathbf{0}$, which is obtained in the previous studies of TOAMD [7], and the corresponding AMD wave functions are reduced to the s -wave states.

B. Description of NN correlations in cluster expansion

In the AMD wave function Φ_{AMD} , there is no explicit description of NN -correlations, and it is energetically unfavorable in nuclei, when there are strong tensor force and short-range repulsion in the bare NN -interaction. In *ab initio* calculations, the NN -correlations are introduced by multiplying the correlation functions to the basis state [10]. In the TOAMD, HMAMD and TO-HMAMD methods, we adopt the AMD wave function as the basis state and treat the correlations between nucleons in terms of the ‘‘cluster expansion’’, where many-body wave function of nuclear system can be expanded into power series of NN -correlations [10, 12]. In Fig. 1, we show the first and second orders of correlation diagrams appearing in the ${}^4\text{He}$ wave functions corresponding to the HMAMD, TOAMD and TO-HMAMD methods, respectively. In these diagrams, the NN -correlations are denoted by connections of particle lines and presented in different colors according to their mathematical descriptions as introduced in the following paragraphs. The column entitled ‘‘[12]’’ contains the two-body diagrams in which only the nucleons labeled ‘‘1’’ and ‘‘2’’ are correlated. The ‘‘[12:23]’’ denotes the connected three-body diagrams with the double product of the NN -correlations connecting ‘‘[12]’’ and ‘‘[23]’’, which belong to the second order in the cluster expansion. The ‘‘[12:34]’’ denotes the disconnected four-body diagrams with the double

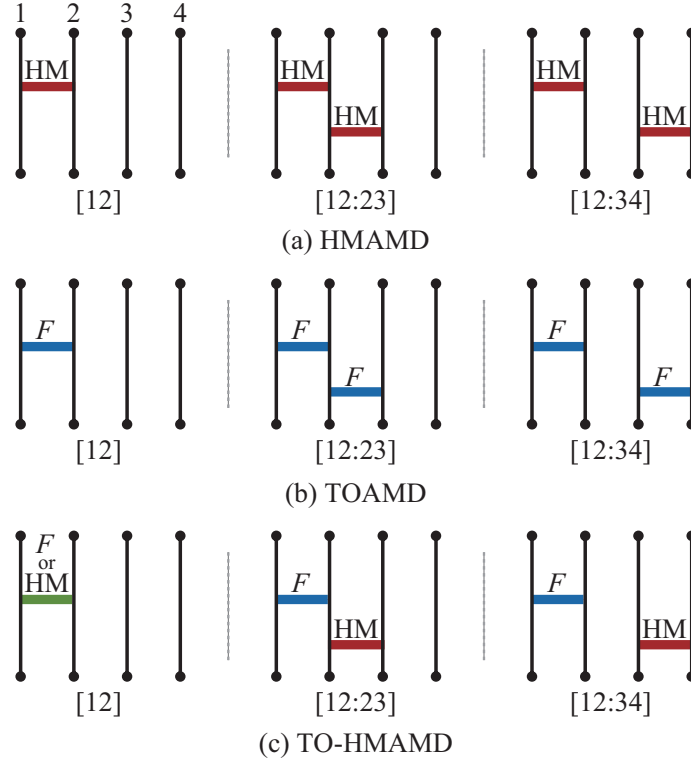


FIG. 1. A part of the correlation diagrams for the ${}^4\text{He}$ wave functions in HMAMD, TOAMD and TO-HMAMD methods. Vertical lines indicate the particles, numbering from the left side as 1, 2, 3, 4. The red connections entitled “HM” denote the NN -correlations described by the high-momentum pairs of nucleons. The blue connections entitled “ F ” denote the NN -correlations described by the TOAMD correlation functions in the central or tensor channels. The green connection entitled “ F or HM” stands for either “ F ” or “HM”. The label with the square bracket below each diagram indicates the configuration of particle correlations.

product of correlations “[12]” and “[34]”. Some other diagrams, such as the ladder term “[12:12]”, are not included in this figure. The cluster expansion in TOAMD approach is explained in detail in Ref. [9].

To obtain the total wave function of nuclei, we superpose the original AMD wave function and the correlated bases described by the diagrams in the cluster expansion, to the first or second order. When only a single NN -correlation such as “[12]” is included in HMAMD and TOAMD method, we call the corresponding methods “single HMAMD” and “single TOAMD”, respectively. When additional second order diagrams with the double product of NN -correlations are also included, these two methods are named “double HMAMD” and

“double TOAMD”, respectively [9, 12]. In the TO-HMAMD method, we include at least first and second order diagrams.

C. High-momentum Antisymmetrized Molecular Dynamics (HMAMD)

In the HMAMD method, the NN correlations are described by introducing high-momentum excitations of nucleon pairs into the AMD wave function, utilizing the imaginary parts of the Gaussian centroids [11, 12, 16, 17]. For s -shell nuclei, we denote the excited pairs according to their spin-isospin combinations:

$$1 : \mathbf{D}_{p\uparrow, n\uparrow}, \quad 2 : \mathbf{D}_{p\uparrow, n\downarrow}, \quad 3 : \mathbf{D}_{n\uparrow, n\downarrow}, \quad 4 : \mathbf{D}_{p\uparrow, p\downarrow}, \quad (3)$$

where the subscripts denote two nucleons in each pair with their spins in the z -direction. The vector symbol \mathbf{D} denotes the imaginary shifts of the Gaussian centroids for the paired nucleons as

$$\begin{aligned} \mathbf{R}_i &\rightarrow \mathbf{R}_i + i\mathbf{D}, \\ \mathbf{R}_j &\rightarrow \mathbf{R}_j - i\mathbf{D}, \end{aligned} \quad (4)$$

where the subscripts i and j denote each nucleon in the NN pair introduced in Eq. (3). The vector \mathbf{D} excites only the relative motion between two nucleons. Both plus and minus signs are included in Eq. (4) to ensure the parity symmetry. The first three cases 1, 2 and 3 in Eq. (3) should be included in the wave function of the ${}^3\text{H}$ nucleus, and the ${}^4\text{He}$ nucleus requires additional case 4. The symmetric spin-isospin states, such as $\mathbf{D}_{p\uparrow, p\uparrow}$, are dropped to ensure the total antisymmetrization for the ground states of s -shell nuclei of which the spatial wave functions are symmetric. This prescription of the correlated pair is extendable to multi-pairs [12].

As discussed in Ref. [11, 12], the imaginary component of the Gaussian centroid $\text{Im}(\mathbf{Z})$ is proportional to the mean value of nucleon momentum as $\langle \mathbf{k} \rangle = 2\nu \cdot \text{Im}(\mathbf{Z})$ in the single-nucleon state described in Eq. (2). The finite \mathbf{D} in Eq. (4) corresponds to a high-momentum excitation of the NN pairs in Eq. (3), hence they are named “high-momentum pairs”. In Ref. [11], we examined the physical role of high-momentum pairs in terms of the shell model. It is found that high-momentum pairs provide the equivalent effect of the full amount of the 2p-2h excitations described in tensor-optimized shell model frameworks [18–22]. It is also

noted that in Ref. [16], they consider two-deuteron model of ${}^4\text{He}$, where one nucleon of each deuteron has a high-momentum component.

In single HMAMD calculations, their bases are formulated by introducing a single high-momentum pair in each AMD basis wave function. The imaginary shift in each high-momentum pair is described in Eq. (4) and the vector \mathbf{D} is selected to be aligned in the spin parallel z - and spin perpendicular x -directions [11]. In the double HMAMD calculations, two high-momentum pairs are additionally introduced in each AMD basis wave function, as shown in the connected and disconnected cases in Fig. 1. As an example of two high-momentum pairs for three nucleons, we show the shifted Gaussian centroids for the connected case [10] as

$$\begin{aligned}\mathbf{R}_i &\rightarrow \mathbf{R}_i + i\mathbf{D}_1 + i\mathbf{D}_2, \\ \mathbf{R}_j &\rightarrow \mathbf{R}_j - i\mathbf{D}_1, \\ \mathbf{R}_k &\rightarrow \mathbf{R}_k - i\mathbf{D}_2,\end{aligned}\tag{5}$$

where i , j and k denote three nucleons with two kinds of the connected high-momentum pairs \mathbf{D}_1 and \mathbf{D}_2 . For the bases with two high-momentum pairs, the z and x -directions are adopted for the first pair and x , y and z -directions are taken for the second pair [12].

Usually, the HMAMD bases are constructed with the good quantum number K for the z -component of total angular momentum. In this case, the rotational symmetry is restored by the projection of basis $|\Psi_{\text{HMAMD}}\rangle$ onto the eigenstates of the total angular momentum J with the operator \hat{P}_{MK}^J [23], as

$$\begin{aligned}|\Psi_{\text{HMAMD},n}^{JM}\rangle &= \hat{P}_{MK}^J |\Psi_{\text{HMAMD},n}\rangle \\ &= \frac{2J+1}{8\pi^2} \int d\Omega D_{MK}^{J*}(\Omega) \hat{R}(\Omega) |\Psi_{\text{HMAMD},n}\rangle,\end{aligned}\tag{6}$$

where J is the quantum number of the total angular momentum, K is the magnetic quantum number in the intrinsic state before rotation $\hat{R}(\Omega)$ of Euler angles Ω , and M is the magnetic quantum number after the projection. Subscript n denotes all the parameters in the HMAMD basis including the spin-isospin channels and imaginary shifts \mathbf{D} for high-momentum pairs. In numerical calculations, the integration over Euler angles are performed with the Gauss-Legendre quadrature algorithm. When K is not a good quantum number for basis $|\Psi_{\text{HMAMD},n}\rangle$, superposition of the basis states with different K could be adopted

after the angular momentum projection, as

$$\begin{aligned} & |\Psi_{\text{HMAMD},n}^{JM}\rangle \\ &= \sum_K c_K \hat{P}_{MK}^J |\Psi_{\text{HMAMD},n}\rangle, \end{aligned} \quad (7)$$

where c_K is the coefficient in the superposition, and determined by the diagonalization of the Hamiltonian matrix with respect to the projected bases $\hat{P}_{MK}^J |\Psi_{\text{HMAMD},n}\rangle$.

After the angular momentum projection, HMAMD bases of different spin-isospin channels and the various imaginary shift vectors \mathbf{D} are superposed with the original AMD basis. It is found that the magnitudes of $|\mathbf{D}|$ ranging from 1 fm to 12 fm with an interval of 1 fm is sufficient in the superposition to provide the converging energy in the single HMAMD calculation [11]. After the superposition, NN correlations in nuclei are described precisely, including the tensor [11] and short-range correlations [12].

One significant advantage of the HMAMD approach is its simplicity in analytical derivations of matrix elements. Due to the fact that all HMAMD bases are merely the Slater determinants of the shifted Gaussians with complex centroids, all the matrix elements in the HMAMD bases have the same analytical form as those of the AMD calculation. Hence, only analytical derivations of the AMD matrix elements are necessary. Meanwhile, the formulation of the HMAMD bases leads to difficulty in numerical calculation, which is mainly caused by the relative angles between two kinds of vectors for imaginary shifts when two high-momentum pairs are included simultaneously in the double HMAMD calculation. For this, six bases corresponding to different combinations of pair directions (x, z for the first pair and x, y, z for the second pair) should be included in model space for each combination of magnitudes $|\mathbf{D}_1|$ and $|\mathbf{D}_2|$, which significantly enlarges the number of bases.

D. Tensor-optimized Antisymmetrized Molecular Dynamics (TOAMD)

In the TOAMD approach, NN correlation functions are formulated explicitly in operator forms and then multiplied successively to the AMD basis [6]. In the lowest order, the single TOAMD wave function is written as:

$$(1 + F_D + F_S) \times |\Psi_{\text{AMD}}\rangle, \quad (8)$$

where the operators F_D and F_S correspond respectively to the tensor and short-range correlations. In practical calculations, they are formulated in the Gaussian expansion form,

$$F_D = \sum_m^{n_G} \sum_t C_{D,m}^t f_{D,m}^t, \quad (9)$$

$$F_S = \sum_m^{n_G} \sum_{t,s} C_{S,m}^{t,s} f_{S,m}^{t,s}, \quad (10)$$

where

$$f_{D,m}^t = \sum_{i<j}^A \exp(-a_{D,m}^t r_{ij}^2) O_{ij}^t r_{ij}^2 S_{12}(\hat{r}_{ij}), \quad (11)$$

$$f_{S,m}^{t,s} = \sum_{i<j}^A \exp(-a_{S,m}^{t,s} r_{ij}^2) O_{ij}^t O_{ij}^s. \quad (12)$$

Here, s and t are used to represent the spin-isospin channels of the correlated two nucleons and $O_{ij}^t = (\boldsymbol{\tau}_i \cdot \boldsymbol{\tau}_j)^t$, $O_{ij}^s = (\boldsymbol{\sigma}_i \cdot \boldsymbol{\sigma}_j)^s$. The vector $\mathbf{r}_{ij} = \mathbf{r}_i - \mathbf{r}_j$ is the relative coordinate between the correlated two nucleons. The subscript m denotes the different range parameters $a_{D,m}^t$ and $a_{S,m}^{t,s}$ in the Gaussian expansion of each channel with the number of n_G . The properties of these correlation functions are discussed in Refs. [8, 9].

In double TOAMD calculations, up to the second order of diagrams are included by using double product of the correlation functions F_S and F_D , as

$$(1 + F_D + F_S + F_S F_S + F_S F_D + F_D F_S + F_D F_D) \times |\Psi_{\text{AMD}}\rangle. \quad (13)$$

Parameters in each correlation function F are determined independently and have different coefficients. Comparing with the double HMAMD method, the double TOAMD approach converges faster to the exact solution with the small number of bases. However, this numerical efficiency relies on the enormous efforts to obtain the analytical derivations of matrix elements coming from the double product of FF in Eq. (13). For instance, when calculating the two-body matrix element $\langle \Phi_{\text{AMD}} | F^\dagger F^\dagger V F F | \Phi_{\text{AMD}} \rangle$ for ${}^4\text{He}$, there are 336 diagrams of up to the four-body terms in the cluster expansion of many-body operator $F^\dagger F^\dagger V F F$ [9]. For each of these diagrams, the analytical formulation of matrix elements needs to be derived. In addition, it takes efforts for the code development.

In Ref. [12], the equivalent results between the correlation functions F and high-momentum pairs are discovered. We compared numerical results from double HMAMD

and double TOAMD calculations using the AV4' central interaction with short-range repulsions. In Appendix, we show explicitly the analytical proof for the equivalence between high-momentum pairs and correlation functions F for the central type of NN -correlation under some specific conditions.

E. Tensor-optimized High-momentum Antisymmetrized Molecular Dynamics (TO-HMAMD)

In order to integrate advantages from both HMAMD and TOAMD methods, and balance between the analytical simplicity and numerical efficiency in *ab initio* calculations, we propose the TO-HMAMD method by hybridizing the HMAMD and TOAMD descriptions of NN -correlations. The correlation diagrams for the TO-HMAMD approach are shown in the bottom panel of Fig. 1. For the first order of diagrams, such as “[12]”, the NN -correlations are described by using either the high-momentum pair with the imaginary shift \mathbf{D} or the TOAMD correlation function F_S or F_D . For the second order diagrams, the NN correlations are described in combination of both the high-momentum nucleon pair and the TOAMD correlation function F . The TO-HMAMD wave function can be expressed in the following form as

$$\begin{aligned}
|\Psi_{\text{TO-HMAMD}}^{JM}\rangle &= \sum_n C_n (1 + F_{D,n} + F_{S,n}) \times \sum_K c_K \hat{P}_{MK}^J |\Psi_{\text{HMAMD},n}\rangle, \\
&= \sum_\mu \tilde{C}_\mu \hat{P}_{MK_\mu}^J \tilde{F}_\mu |\Psi_{\text{HMAMD},\mu}\rangle \\
&= \sum_\mu \tilde{C}_\mu \hat{P}_{MK_\mu}^J |\Psi_{\text{TO-HMAMD},\mu}\rangle,
\end{aligned} \tag{14}$$

where $|\Psi_{\text{HMAMD},n}\rangle$ are HMAMD bases with a single high-momentum pair and F_D and F_S are the correlation functions in Eq. (9). The operator \hat{P}_{MK}^J represents the angular momentum projection and c_K is the corresponding superposition coefficients for the quantum number K , as in Eq. (7). For the study of the ${}^4\text{He}$ nucleus in the present work, the HMAMD bases $|\Psi_{\text{HMAMD},n}\rangle$ are constructed with the good quantum number K in the intrinsic frame, and the summation over K reduces to a single term with $K = 0$. Subscripts n for the correlation functions F_D and F_S indicate that parameters in $F_{D,n}$ and $F_{S,n}$ are determined independently for each HMAMD basis $|\Psi_{\text{HMAMD},n}\rangle$. The operator \tilde{F}_μ in the second line is selected from the operators $\{1, f_{D,m}^t, f_{S,m}^{t,s}\}$ that correspond to three different channels

where $f_{D,m}^t$ and $f_{S,m}^{t,s}$ are defined in Eqs. (11) and (12). The subscripts μ denote all the adjustable parameters, including the quantum number K_μ , the spin-isospin combination and the imaginary shift \mathbf{D} (including $\mathbf{0}$) of high-momentum pairs in $|\Psi_{\text{HMAMD},n}\rangle$, and the quantum numbers for spin s and isospin t , and the Gaussian range parameter m of the operator \tilde{F} . $|\Psi_{\text{TO-HMAMD},\mu}\rangle = \tilde{F}_\mu |\Psi_{\text{HMAMD},\mu}\rangle$ are defined as TO-HMAMD bases and \tilde{C}_μ are the corresponding expansion coefficients. Then, the energy and wave function of a nucleus could be obtained by solving the Hill-Wheeler equation, as

$$\sum_{\mu,\mu'} (H_{\mu\mu'} - EN_{\mu\mu'}) \tilde{C}_{\mu'} = 0, \quad (15)$$

where $H_{\mu\mu'}$ and $N_{\mu\mu'}$ are the Hamiltonian and norm matrix elements, respectively, as

$$H_{\mu\mu'} = \langle \Psi_{\text{TO-HMAMD},\mu} | \hat{P}_{MK_\mu}^{J\dagger} H \hat{P}_{MK_{\mu'}}^J | \Psi_{\text{TO-HMAMD},\mu'} \rangle, \quad (16)$$

$$N_{\mu\mu'} = \langle \Psi_{\text{TO-HMAMD},\mu} | \hat{P}_{MK_\mu}^{J\dagger} \hat{P}_{MK_{\mu'}}^J | \Psi_{\text{TO-HMAMD},\mu'} \rangle. \quad (17)$$

In the above matrix elements, the integrations over the Euler angles Ω in $\hat{P}_{MK_\mu}^J$ are performed numerically but the integral kernels such as $\langle \Psi_{\text{TO-HMAMD},\mu} | H | \Psi_{\text{TO-HMAMD},\mu'} \rangle$ are obtained analytically. As discussed in Subsection II C, the introduction of high-momentum pairs does not require the additional components of the analytical forms of matrix elements. Hence, in analytical derivations of the matrix elements, $\langle \Psi_{\text{TO-HMAMD},\mu} | H | \Psi_{\text{TO-HMAMD},\mu'} \rangle$ is reduced to the matrix element $\langle \Psi_{\text{TOAMD},\mu} | H | \Psi_{\text{TOAMD},\mu'} \rangle$ for the single TOAMD wave function, which is to be obtained in term of the cluster expansion [9]. As an example, in Fig. 2 we show 16 diagrams in the cluster expansion associated to the two-body operator V , in the order of V (a), $F^\dagger V$ (b-d) and $F^\dagger V F$ (e-p) cases. The integral kernels corresponding to each diagram should be derived analytically.

We get now three methods for the treatment of the correlations among nucleons. In Table I, we compare the analytical and numerical efforts in detail for the new TO-HMAMD method as compared with the double HMAMD and double TOAMD approaches. The second row lists the numbers of diagrams in the cluster expansions that need to be derived analytically in the calculation of matrix elements for the two-body operator V . In the double HMAMD approach, high-momentum pairs do not change the analytical form of matrix element. Therefore, all the diagrams are reduced to the most simple type as shown in Fig. 2 (a), and only one integral kernel for operator V is to be derived analytically. In the double TOAMD method, the number of diagrams is 412, including 16 diagrams shown in

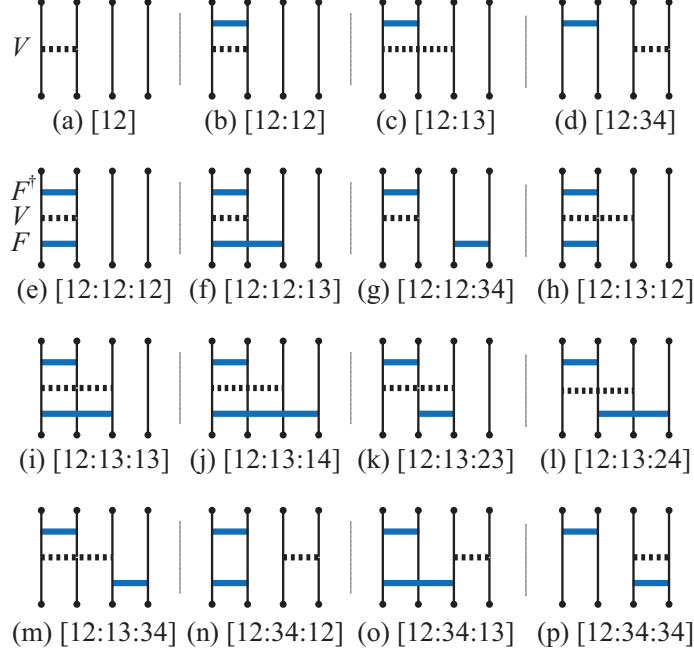


FIG. 2. Diagrams of cluster expansions in calculating matrix elements for the two-body operator V . The diagram (a) is for the operator V . The diagrams (b-d) correspond to the cluster expansion of the operator $F^\dagger V$. The diagrams (e-p) correspond to the cluster expansion of the operator $F^\dagger V F$. The blue connections indicate the TOAMD correlation functions F_D or F_S . The dotted connections indicate the two-body operator V . For each diagram, the corresponding integral kernels should be derived analytically.

Fig. 2, 60 diagrams for $F^\dagger V F F$ and 336 diagrams for $F^\dagger F^\dagger V F F$, as discussed in Ref. [9]. The integral kernel corresponding to each of these diagrams needs to be derived independently. In the new hybridized TO-HMAMD method, the diagrams are reduced to 16 different single TOAMD diagrams as shown in Fig. 2, which significantly simplifies the analytical derivation, comparing with the double TOAMD case. It is therefore clearly shown that in the calculation of the two-body operator V , TO-HMAMD requires more analytical efforts comparing to double HMAMD, but provides significantly simpler mathematical framework than that of double TOAMD.

Another advantage in the TO-HMAMD approach is that only the z -direction of the imaginary shift \mathbf{D} is necessary in the HMAMD part [5]. This is because of the fact that the relative coordinates \mathbf{r} between the correlated two nucleons is integrated over the entire space by using the correlation functions of F_D and F_S in Eqs. (9) and (10), which contribute to

TABLE I. The comparison of analytical and numerical settings between the double HMAMD, double TOAMD and TO-HMAMD methods in the calculation of ${}^4\text{He} (0^+)$. In the first row, we compare the number of diagrams in calculating matrix elements for the two-body operator V . For each diagram, the corresponding integration kernels should be derived analytically. In the second and third rows, we compare the number of bases in the superposition and the number of mesh points in numerical integrations for the angular momentum projection (AP). The numbers of bases for double HMAMD and double TOAMD are the estimated ones. The definitions of the diagrams and bases are explained in the text and in Fig. 2.

	Double	Double	TO-
	HMAMD	TOAMD	HMAMD
Diagrams Number	1	412 [9]	16
Bases Number	13824	1369	1813
AP mesh points Number	8000 [12]	–	14

the high-momentum excitations for the NN -pairs in any direction. Hence, all the possible relative angles between the two kinds of the correlated NN -pairs, described respectively by the high-momentum pairs and $F_{D,S}$, are naturally taken into account. Consequently, the number of bases are significantly smaller in the TO-HMAMD method comparing to the double HMAMD approach, where different directions of momenta in the first and second high-momentum pairs should be taken into account.

In the third row of Table I, we compare the number of bases that is required in the numerical calculations among the TO-HMAMD, double HMAMD and double TOAMD methods. The basis number for the double HMAMD calculation is estimated as follows. We set $n_D=12$ with different magnitudes for the imaginary shifts \mathbf{D} in two directions (x and z) for both the first and second pairs and select two sets among four kinds of spin-isospin combinations in Eq. (3). The parity doublets for these pairs are also included. The total base number is then estimated to be $(n_D \times 2 \times 2)^2 \times C(4, 2) = 13824$. For the double TOAMD method, we typically include $n_G=6$ of different ranges in Gaussian expansion for each of the 6 channels of the correlation function F in Eqs. (9) and (10), and then the total number of bases could be approximated by $(1+6 \times n_G)^2 = 1369$. In TO-HMAMD, we adopt all the 4 possible spin-isospin

combinations in Eq. (3) for each high-momentum pair in the HMAMD bases $|\Psi_{\text{HMAMD}}\rangle$ in Eq. (14). Each pair is fixed in the z direction with $n_{\text{D}} = 6$ different magnitudes of the imaginary shift and their parity doublets are also included. In the correlation functions F in Eq. (14), we include for each of the 6 channels $n_{\text{G}} = 6$ proper ranges for the Gaussian expansion. Hence the total number of TO-HMAMD bases is $(1 + 4 \times 2 \times n_{\text{D}}) \times (1 + 6 \times n_{\text{G}}) = 1813$. It is observed that the number of bases in TO-HMAMD is similar to that in double TOAMD but much smaller than that in double HMAMD method. From this fact, we conclude that the numerical efficiencies of TO-HMAMD and double TOAMD in describing the exact wave function are better as compared to the double HMAMD method.

In the application to the 0^+ ground state of ${}^4\text{He}$, there is one additional advantage in the TO-HMAMD approach. In this state, the TO-HMAMD wave function has the rotational symmetry around the z -axis and hence the angular momentum projection operator \hat{P}_{MK}^J in Eq. (14) reduces to

$$\hat{P}_{00}^0 = \frac{1}{8\pi^2} \int d\beta \sin \beta \hat{R}(\beta), \quad (18)$$

where the rotation over the Euler angles $\Omega = \{\alpha, \beta, \gamma\}$ is reduced to a single rotation over the polar angle β . This reduces significantly the numerical efforts because the integration over the angle α and γ can be skipped. In the TO-HMAMD calculation of ${}^4\text{He}(0^+)$, we adopt 14 mesh points in the numerical integration over the angle β . This reduction of the effort for the angular momentum projection is only valid for the calculation of the 0^+ states and it is not available for the calculation of ${}^3\text{H}$ nucleus, the ground state of which has the spin-parity $1/2^+$. In addition, this reduction relies on the rotational symmetry around z -axis, which is broken in the double HMAMD wave function by the high-momentum pairs in the x -direction. Hence, in this case the numerical integration has to be carried out for all of the three Euler angles. In the previous double HMAMD calculation, the total number of mesh points for the projection is $20 \times 20 \times 20 = 8000$ [12]. In the fourth row of Table I, we compare the total number of mesh points for the angular momentum projection between the double HMAMD and TO-HMAMD calculations, which further illustrate the numerical efficiency in the TO-HMAMD approach. In addition, we note that the double TOAMD wave function has the intrinsic spin-parity 0^+ for the ground state of ${}^4\text{He}$, because of the scalar nature of the correlation functions F in Eqs. (9) and (10). Therefore, the angular momentum projection is not necessary for the double TOAMD method.

As a balance between the analytical and numerical simplicity, the TO-HMAMD approach

can be extended to the p -shell nuclei with minimal efforts, which makes it a promising *ab initio* method in the p -shell nuclear system.

III. RESULTS FOR THE ${}^4\text{He}$ NUCLEUS

We perform the *ab initio* calculation of the ${}^4\text{He}$ nucleus with the TO-HMAMD method using the AV8' bare interaction. The Gaussian range parameter ν in Eq. (1) is variationally optimized as $\nu=0.20\text{ fm}^{-2}$. The corresponding energy curve of ${}^4\text{He}$ by successively adding high-momentum pairs, and correlation functions F_D and F_S are presented in Fig. 3. It is observed that both the additions of high-momentum pairs and correlation functions $F_{S,D}$ significantly improve the total energy of ${}^4\text{He}$, and the final TO-HMAMD result converges with the double TOAMD calculation.

In Fig. 4 and Table II, we show the evolution of the Hamiltonian components and the radius of ${}^4\text{He}$ with the successive addition of high-momentum pairs and correlation functions. We found that both the central (red curve) and tensor (green curve) terms are improved by the first inclusion of high-momentum pairs, especially for the central term where the improvement is as large as 48.8 MeV. This means that both the tensor and short-range correlations are treated by using high-momentum pairs. It is interesting that the spin-orbit term remains almost 0 MeV for the AMD case, showing that the spin-orbit correlation can

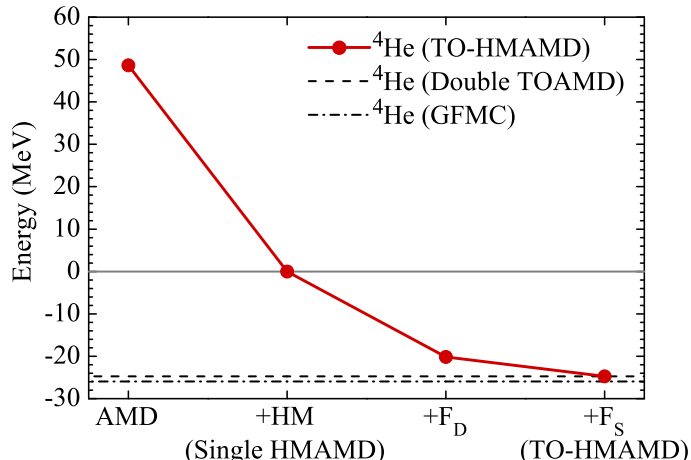


FIG. 3. The energy of the ${}^4\text{He}$ nucleus calculated with TO-HMAMD using the bare interaction AV8' by successively adding the high-momentum pairs (+HM), and correlation functions F_D and F_S .

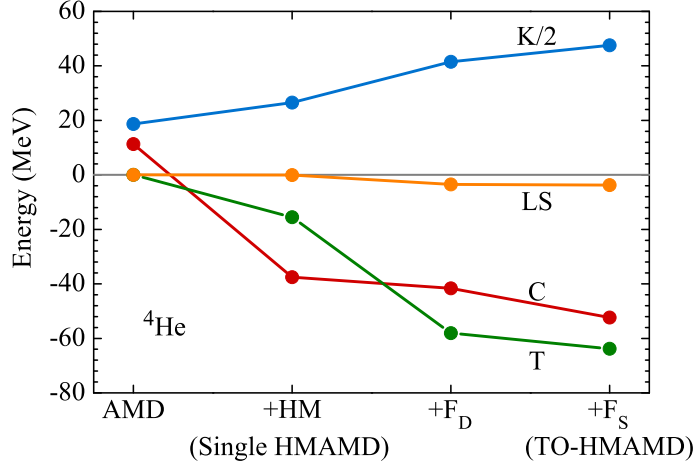


FIG. 4. Hamiltonian components of the ${}^4\text{He}$ nucleus calculated with TO-HMAMD using the bare interaction $\text{AV8}'$ by successively adding the high-momentum pairs (+HM), and correlation functions F_D and F_S . “K/2” denotes a half of kinetic component. “C”, “T” and “LS” denote central, tensor and spin-orbit components, respectively.

TABLE II. Total energies, Hamiltonian components and root-mean-square radii of ${}^4\text{He}$ (0^+) calculated with TO-HMAMD using the bare interaction $\text{AV8}'$ by successively adding the high-momentum pairs (+HM), and correlation functions F_D and F_S . The units of energies and radii are MeV and fm, respectively.

	AMD	+HM	+ F_D	+ F_S
Energy	48.64	-0.01	-20.14	-24.74
Kinetic	37.32	53.11	82.99	95.17
Central	11.31	-37.50	-41.61	-52.33
Tensor	0.00	-15.55	-58.05	-63.80
LS	0.00	-0.07	-3.47	-3.77
Radius	1.68	1.71	1.58	1.51

only be well described by the second order of correlation diagrams. In the next introduction of tensor correlation function F_D , the tensor term is more significantly improved by 42.5 MeV comparing to the central term. In addition, contribution of the spin-orbit term arises with a finite value -3.46 MeV as expected, because of the coupling between the high-momentum pair and tensor correlation function F_D . The addition of the last correlation

function F_S contributes to all the Hamiltonian components. For each addition of high-momentum pairs and correlation functions, we observe significant increases of the kinetic energy, which correspond to the high-momentum excitations induced by the short-range repulsion and tensor attraction in the AV8' bare interaction.

TABLE III. Total energies, Hamiltonian components and root-mean-square radius of ${}^4\text{He}$ (0^+) calculated with TO-HMAMD using AV8' potential in comparison with the TOAMD and GFMC methods. “ F^2 -TOAMD” denotes the double TOAMD method. The units of energies and radii are MeV and fm, respectively.

	TO-HMAMD	F^2 -TOAMD[9]	GFMC[24]
Energy	-24.74	-24.74	-25.93
Kinetic	95.17	97.06	102.3
Central	-52.33	-53.12	-55.05
Tensor	-63.80	-64.84	-68.05
LS	-3.77	-3.83	-4.75
Radius	1.51	1.50	1.49

We compare the TO-HMAMD results of the ${}^4\text{He}$ nucleus with the double TOAMD and GFMC methods by listing the total energy, Hamiltonian components and the root-mean-square radius obtained from each method in Table III. Nice agreements are found for each component between the TO-HMAMD and other two methods. The TO-HMAMD method is found to reproduce exactly the same total energy of ${}^4\text{He}$ nucleus as the double TOAMD calculation, showing that these two methods describe almost the same wave function. Comparing with the double TOAMD results, the kinetic energy in TO-HMAMD results is slightly smaller. This indicates that the high-momentum components are slightly underestimated in the current calculation. When the TO-HMAMD calculation is performed with larger model space, it is expected that small difference between current result and precise solution can be further reduced.

IV. SPIN-ISOSPIN CHANNEL DEPENDENCE OF THE NN -CORRELATION

We further discuss the spin-isospin channel dependence of NN -correlations in both descriptions using high-momentum pairs or correlation functions F . In Fig. 5, we show the spin-isospin channel dependence for the NN -correlations described by the correlation function F in the single TOAMD and TO-HMAMD calculations of ${}^4\text{He}$. In this figure, we project the correlation functions F_S and F_D in Eqs. (9) and (10) into spin-isospin eigenstates of the correlated two nucleons, and add these correlation functions successively in the order of triplet-even (TE), singlet-even (SE), triplet-odd (TO) and singlet-odd (SO) channels. As shown by the red curve in Fig. 5, which corresponds to the single TOAMD calculation, the even channels contribute to the entire energy improvements from the AMD basis, while the odd channels have exactly no effect. This originates from the total even parity of the s -wave AMD basis state of ${}^4\text{He}$, and single correlation function F should be in the even channel to preserve the parity of the AMD basis state. In the case of the TO-HMAMD calculation (green curve), we observe a similar dominance of the even channels. However, in this case, contributions from the odd channels are very small but finite, because of the coupling terms between odd TOAMD correlation functions and odd channels of high-momentum pairs. Furthermore, the triplet-even channel contributes to about 95% of the total energy improvement, which agrees with the prediction from the one-pion-exchange process [25]. In

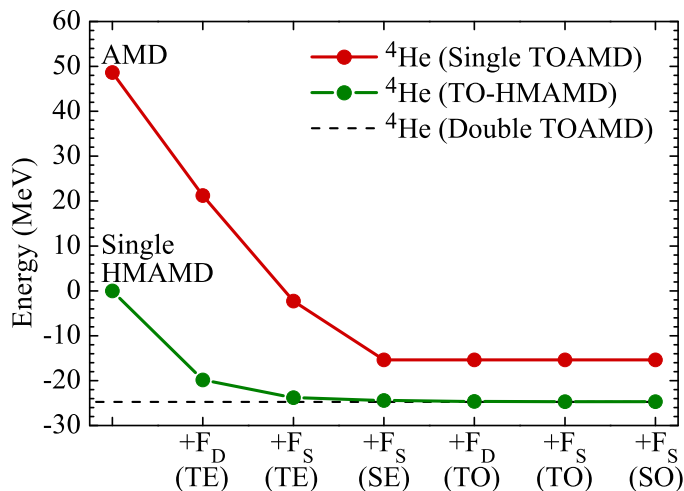


FIG. 5. The energy convergence of ${}^4\text{He}$ with respect to the spin-isospin channels of the correlation functions F_D and F_S in TO-HMAMD and single TOAMD calculations.

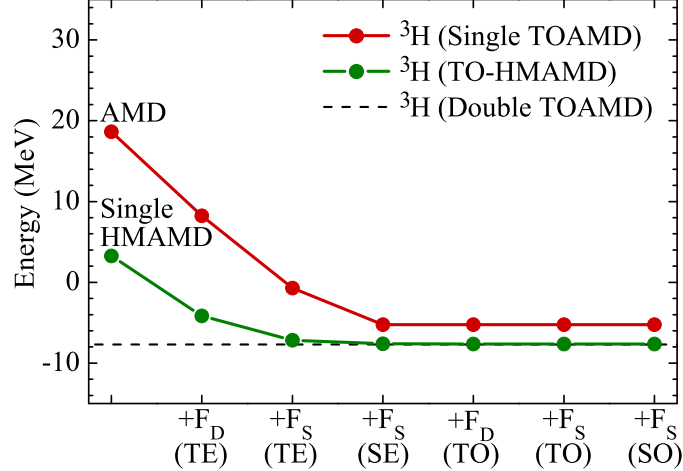


FIG. 6. The energy convergence of ${}^3\text{H}$ with respect to the spin-isospin channels of the correlation functions F_D and F_S in TO-HMAMD and single TOAMD calculations.

Fig. 6, we show similar channel dependence of the correlation functions F in the ${}^3\text{H}$ nucleus where total energy is obtained as -7.64 MeV with the AV8' interaction.

The NN -correlation is also described by the high-momentum pairs of nucleons in the TO-HMAMD calculation. In Fig. 7, we show the energy contribution from each successive addition of various spin-isospin combinations for the high-momentum pairs in Eq. (3). It is found that in both single HMAMD and TO-HMAMD calculations, the $(p \uparrow, n \uparrow)$ high-momentum pairs contribute to the most of the energy improvements comparing with the original AMD or the single TOAMD basis. On the other hand, $(n \uparrow, n \downarrow)$ and $(p \uparrow, p \downarrow)$ pairs have a smaller contribution to the total energy, especially in the TO-HMAMD calculations. Considering that the $(p \uparrow, n \uparrow)$ pair contains both the triplet-even and triplet-odd channels, while $(n \uparrow, n \downarrow)$ and $(p \uparrow, p \downarrow)$ pairs contain only triplet-odd but no triplet-even channels, we may conclude that the triplet-even channel also dominates the NN -correlations in the description using the high-momentum pairs, as the previous discussions for the correlation functions F . The similar spin-isospin dependence is also shown for the ${}^3\text{H}$ nucleus in Fig. 8. We also notice that the contributions from the $(n \uparrow, n \downarrow)$ and $(p \uparrow, p \downarrow)$ pairs are finite in Fig. 8 instead of the negligible results reported in Ref. [11]. This is because of the fact that the $(n \uparrow, n \downarrow)$ and $(p \uparrow, p \downarrow)$ pairs improve descriptions of short-range correlations induced by the AV8' interaction in this calculation, while for the calculation in Ref. [11], no short-range repulsion is included in the central interaction.

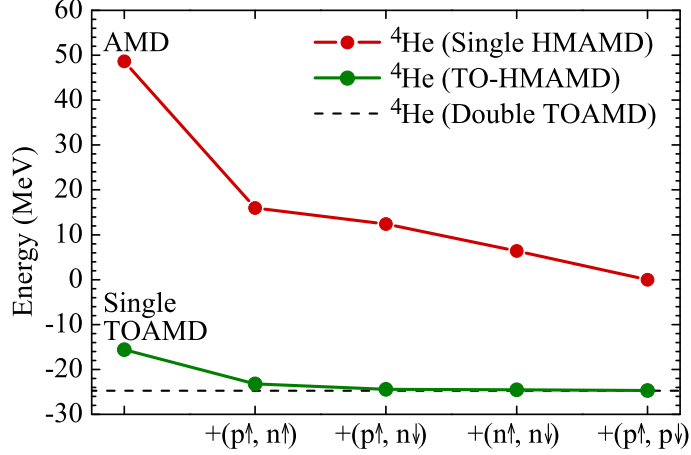


FIG. 7. Energy convergence of ${}^4\text{He}$ with respect to the spin-isospin combinations of the high-momentum pairs in TO-HMAMD and single HMAMD calculations.

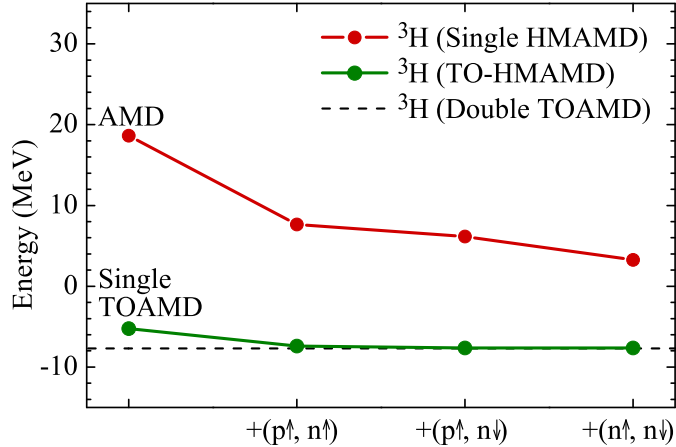


FIG. 8. Energy convergence of ${}^3\text{H}$ with respect to the spin-isospin combinations of the high-momentum pairs in TO-HMAMD and single HMAMD calculations.

In future *ab initio* calculations with the TO-HMAMD method, the information of the dependence on the spin-isospin channel can be utilized for more effective description of NN -correlations in nuclei.

V. CONCLUSION

In conclusion, we propose the variational “TO-HMAMD” framework for *ab initio* calculation of nuclei by hybridizing the tensor-optimized and high-momentum AMD approaches (TOAMD and HMAMD). The wave function of nuclei is formulated by using the AMD ref-

erence state and the additional NN -correlations expressed in the form of cluster expansion. The correlation diagrams are included up to the second order and described by the product of high-momentum pairs and spatial correlation functions. Comparing with other two methods based on AMD (double HMAMD and double TOAMD), it is found that the newly proposed TO-HMAMD approach has an advantage in balancing analytical simplicity and numerical efficiency, which is ideal for the future extensions to p -shell nuclei. Through the TO-HMAMD approach, the ${}^4\text{He}$ nucleus is calculated using the AV8' bare interaction. It is found that the total energy, Hamiltonian components and root-mean-square radius of the ${}^4\text{He}$ nucleus are well reproduced comparing to the double TOAMD and GFMC results. We also discuss the spin-isospin channel dependence of NN -correlations in TO-HMAMD, and observe the dominance of even channels, especially the triplet-even channel, in the description of NN correlations within the ground state of ${}^4\text{He}$. In future studies, the application of the TO-HMAMD approach will be extended to p -shell and heavier nuclear systems. Because of its flexibility in describing the NN -correlations and its advantages in analytical and numerical efficiency, it is expected that the TO-HMAMD can be used as a general *ab initio* framework for the p -shell nuclear systems.

ACKNOWLEDGMENTS

M.L. acknowledges the support from the RCNP theoretical group for his stay in RCNP and the fruitful discussions with the members, and the support from the Yozo Nogami Research Encouragement Funding. This work was supported by the JSPS KAKENHI Grants No. JP18K03660, No. JP15K05091, No. JP15K17662, and No. JP16K05351. One of the authors (M.I.) is supported by the Grants-in-Aid for Young Scientists (B) (No. 15K17671) and Grant-in-Aid for JSPS Research Fellow (No. 16J05297). The numerical calculations were performed on the high performance computing server at RCNP, Osaka University.

Appendix: Comparison between HMAMD and TOAMD

We compare single HMAMD and single TOAMD wave functions for the central-type correlation. The single HMAMD wave function with an imaginary shift \mathbf{D} is written as

$$\Psi_{\text{HMAMD}}^{J\pi}(\mathbf{D}) = \sum_{i<j}^A C_{ij} P^{J\pi} \mathcal{A} \left\{ \phi_i(\mathbf{r}_i, i\mathbf{D}) \phi_j(\mathbf{r}_j, -i\mathbf{D}) \cdot \prod_{p \neq i,j}^{A-2} \phi_p(\mathbf{r}_p) \right\}, \quad (\text{A.1})$$

where \mathcal{A} is an antisymmetrizer. ϕ_i , ϕ_j and ϕ_p are single-nucleon states, where ϕ_i and ϕ_j have imaginary shifts $\pm i\mathbf{D}$ as shown in Eq. (2) and ϕ_p is a single-nucleon state expressed by Eq. (1). $P^{J\pi}$ denotes the angular momentum and parity projections.

When only the central correlation F_S is included, for one Gaussian function term of F_S in Eq. (10) with the range parameter a , we can express the corresponding single TOAMD wave function as

$$\Psi_{\text{TOAMD}} = F_S \Psi_{\text{AMD}} \quad (\text{A.2})$$

$$= \sum_{i<j}^A f_{ij} P^{J\pi} \mathcal{A} \left\{ \prod_{p=1}^A \phi_p(\mathbf{r}_p) \right\}, \quad (\text{A.3})$$

where the pair function is $f_{ij} = e^{-a(\mathbf{r}_i - \mathbf{r}_j)^2}$.

We consider two assumptions in HMAMD below:

1. Superpose all the basis states having high-momentum pairs with an equal weight, namely, $C_{ij} = 1$.
2. Integrate over the vector \mathbf{D} corresponding to the momentum, with the Gaussian weight with the range b , namely,

$$\Psi_{\text{HMAMD}}^{J\pi} = \int d\mathbf{D} e^{-b\mathbf{D}^2} \Psi_{\text{HMAMD}}(\mathbf{D}) \quad (\text{A.4})$$

Under these assumptions, we consider the relation between the wave functions of HMAMD and TOAMD. The integrated HMAMD wave function can be expressed as

$$\Psi_{\text{HMAMD}}^{J\pi} = \int d\mathbf{D} e^{-b\mathbf{D}^2} \sum_{i<j}^A P^{J\pi} \mathcal{A} \left\{ \phi_i(\mathbf{r}_i, i\mathbf{D}) \phi_j(\mathbf{r}_j, -i\mathbf{D}) \prod_{p \neq i,j}^{A-2} \phi_p(\mathbf{r}_p) \right\} \quad (\text{A.5})$$

For the s -wave configuration, we limit the case of $\mathbf{R} = \mathbf{0}$ for all real components of centroid \mathbf{R} for ϕ_i , ϕ_j and ϕ_p . Hence from Eq. (2), we have the relation

$$\phi_i(\mathbf{r}_i, i\mathbf{D}) \phi_j(\mathbf{r}_j, -i\mathbf{D}) = \phi_i(\mathbf{r}_i) \phi_j(\mathbf{r}_j) \times e^{2i\nu\mathbf{D} \cdot (\mathbf{r}_i - \mathbf{r}_j)} e^{2\nu\mathbf{D}^2}, \quad (\text{A.6})$$

and substitute this relation into the single HMAMD wave function as

$$\Psi_{\text{HMAMD}}^{J\pi} = \sum_{i<j}^A P^{J\pi} \mathcal{A} \left\{ \int d\mathbf{D} e^{-b\mathbf{D}^2} e^{2i\nu\mathbf{D}\cdot(\mathbf{r}_i-\mathbf{r}_j)} e^{2\nu\mathbf{D}^2} \prod_p^A \phi_p(\mathbf{r}_p) \right\} \quad (\text{A.7})$$

$$= \sum_{i<j}^A P^{J\pi} \mathcal{A} \left\{ e^{-a'(\mathbf{r}_i-\mathbf{r}_j)^2} \cdot \prod_p^A \phi_p(\mathbf{r}_p) \right\} \quad (\text{A.8})$$

where $a' = \frac{\nu^2}{b-2\nu}$. Considering b is an adjustable parameter, we may choose an appropriate b to obtain $a' = a$ using a pair function f_{ij} , and

$$\Psi_{\text{HMAMD}}^{J\pi} = \sum_{i<j}^A P^{J\pi} \mathcal{A} \left\{ f_{ij} \prod_p^A \phi_p(\mathbf{r}_p) \right\} \quad (\text{A.9})$$

$$= \sum_{i<j}^A P^{J\pi} \sum_p \epsilon(P) f_{P_i P_j} \cdot \phi_1(\mathbf{r}_{P_1}) \phi_2(\mathbf{r}_{P_2}) \cdots \phi_A(\mathbf{r}_{P_A}) \quad (\text{A.10})$$

$$= P^{J\pi} \sum_p \epsilon(P) \left(\sum_{i<j}^A f_{P_i P_j} \right) \phi_1(\mathbf{r}_{P_1}) \phi_2(\mathbf{r}_{P_2}) \cdots \phi_A(\mathbf{r}_{P_A}). \quad (\text{A.11})$$

Here, $\epsilon(P)$ is a sign for the permutation P as

$$P : \begin{pmatrix} 1 & 2 & \cdots & A \\ P_1 & P_2 & \cdots & P_A \end{pmatrix}. \quad (\text{A.12})$$

From the symmetry of f_{ij} we have the following relation

$$\sum_{i<j}^A f_{P_i P_j} = \sum_{i<j}^A f_{ij}. \quad (\text{A.13})$$

Hence, this scalar factor can be factorized from the antisymmetrization and J^π projection operator as

$$\Psi_{\text{HMAMD}}^{J\pi} = \sum_{i<j}^A f_{ij} \cdot P^{J\pi} \cdot \mathcal{A} \left\{ \prod_p^A \phi_p(\mathbf{r}_p) \right\} \quad (\text{A.14})$$

$$= F_S \Psi_{\text{AMD}} \quad (\text{A.15})$$

$$= \Psi_{\text{TOAMD}}. \quad (\text{A.16})$$

With this equation, we have shown the equivalence of the wave functions of the single HMAMD and single TOAMD for the s -wave configuration under the above two conditions.

REFERENCES

- [1] S. C. Pieper and R. B. Wiringa, *Annu. Rev. Nucl. Part. Sci.* **51**, 53 (2001).
- [2] N. Ishii, S. Aoki, and T. Hatsuda, *Phys. Rev. Lett.* **99**, 022001 (2007).
- [3] S. C. Pieper, V. R. Pandharipande, R. B. Wiringa, and J. Carlson, *Phys. Rev. C* **64**, 014001 (2001).
- [4] T. Neff and H. Feldmeier, *Nucl. Phys.* **A713**, 311 (2003).
- [5] M. Lyu, M. Isaka, T. Myo, H. Toki, K. Ikeda, H. Horiuchi, T. Suhara, and T. Yamada, *Prog. Theor. Exp. Phys.* **2018**, 011D01 (2018).
- [6] T. Myo, H. Toki, K. Ikeda, H. Horiuchi, T. Suhara, *Prog. Theor. Exp. Phys.* **2015**, 073D02 (2015).
- [7] T. Myo, H. Toki, K. Ikeda, H. Horiuchi, T. Suhara, *Phys. Lett. B* **769**, 213 (2017).
- [8] T. Myo, H. Toki, K. Ikeda, H. Horiuchi, T. Suhara, *Phys. Rev. C* **95**, 044314 (2017).
- [9] T. Myo, H. Toki, K. Ikeda, H. Horiuchi, T. Suhara, *Prog. Theor. Exp. Phys.* **2017**, 073D01 (2017).
- [10] T. Myo, H. Toki, K. Ikeda, H. Horiuchi, and T. Suhara, *Phys. Rev. C* **96**, 034309 (2017).
- [11] T. Myo, H. Toki, K. Ikeda, H. Horiuchi, T. Suhara, M. Lyu, M. Isaka, and T. Yamada, *Prog. Theor. Exp. Phys.* **2017**, 111D01 (2017).
- [12] T. Myo, *Prog. Theor. Exp. Phys.* **2018**, 031D01 (2018).
- [13] M. Isaka et al., *to be submitted*.
- [14] Y. Kanada-En'yo, M. Kimura and H. Horiuchi, *C. R. Phys.* **4**, 497 (2003).
- [15] Y. Kanada-En'yo, M. Kimura and A. Ono, *Prog. Theor. Exp. Phys.* **2012**, 01A202 (2012).
- [16] N. Itagaki and A. Tohsaki, *Phys. Rev. C* **97**, 014304 (2018).
- [17] H. Matsuno, Y. Kanada-Enyo, and N. Itagaki, [arXiv:1805.10087](https://arxiv.org/abs/1805.10087) [nucl-th] (2018).
- [18] T. Myo, K. Katō, and K. Ikeda, *Prog. Theor. Phys.* **113**, 763 (2005)
- [19] T. Myo, S. Sugimoto, K. Katō, H. Toki, and K. Ikeda, *Prog. Theor. Phys.* **117**, 2007 (257)
- [20] T. Myo, K. Katō, H. Toki, and K. Ikeda, *Phys. Rev. C* **76**, 024305 (2007)
- [21] T. Myo, H. Toki and K. Ikeda, *Prog. Theor. Phys.* **121**, 511 (2009)
- [22] T. Myo, A. Umeya, H. Toki, and K. Ikeda, *Phys. Rev. C* **84**, 034315 (2011)

- [23] P. Ring and P. Schuck, *The Nuclear Many-Body Problem* (Springer-Verlag, New York, 1980).
- [24] H. Kamada et al., Phys. Rev. C **64**, 044001 (2001) and the references therein.
- [25] J. Carlson and R. Schiavilla, Rev. Mod. Phys. **70**, 743 (1998).